# Membrane fouling mitigation during enhanced coagulation membrane filtration via zero valent iron (ZVI) addition to treat micro-polluted surface water

Xinfei Guo[a], Dongliang Liu[a], Cong Ma[a,b,*], Jie Wang[a], Hongwei Zhang[a]

[a]State Key Laboratory of Separation Membranes and Membrane Processes, School of Environmental and Chemical Engineering, Tianjin Polytechnic University, Tianjin 300387, China, Tel. +86 22 83955883; email: feifei_0630@sina.com (X.F. Guo), Tel. +86 13012251021; email: 13012251021@163.com (D.L. Liu), Tel. +86 22 83955883; email: macong_0805@126.com (C. Ma), Tel. +86 22 83955668; email: wangjie@tjpu.edu.cn (J. Wang), Tel. +86 22 83955666; email: hwzhang@tju.edu.cn (H.W. Zhang)
[b]Department of Chemical and Biomolecular Engineering, University of Connecticut, 191 Auditorium Road, Unit 3222, Storrs, CT 06269-3222, USA

### ABSTRACT

Despite being a promising water treatment technology, membrane filtration still suffers from membrane fouling issues that represent a major disadvantage for membrane applications. This study was aimed to mitigate membrane fouling via addition of zero valent iron (ZVI, $Fe^0$) to a conventional coagulation (ZVI–coagulation) in combination with a membrane treatment of micro-polluted surface water. By determining the characteristic indexes of micro-polluted surface waters (i.e., total organic carbon, chemical oxygen demand [$COD_{Mn}$], and $UV_{254}$), 6 mg/L was revealed to be the optimal ZVI dosage, leading to higher removal efficiencies for these indexes (5.4, 13.7, and 23.1%, respectively) as compared with the conventional coagulation process. Additionally, after three operation cycles, the herein developed ZVI–coagulation membrane process showed higher final normalized flux ($J/J_0$) values as compared with the conventional coagulation membrane technology (0.38 vs. 0.24, respectively). As revealed by fluorescence excitation–emission matrix, X-ray diffraction, and scanning electron microscopy analyses, ZVI was highly efficient in removing membrane fouling contaminants such as protein-like substances and organic matters during the filtration process. Furthermore, the addition of ZVI seemed to positively influence the floc and cake layer characteristics of the membrane. Thus, the addition of ZVI resulted in larger and looser flocs and looser and more permeable cake layers. We demonstrated that the ZVI–coagulation membrane combined filtration process represents a promising approach to enhance coagulation and mitigate membrane fouling during the treatment of micro-polluted surface waters.

*Keywords:* Zero valent iron (ZVI); Water treatment; Enhanced coagulation; Membrane fouling; Micro-polluted surface water

## 1. Introduction

Low-pressure membrane filtration technologies such as microfiltration and ultrafiltration have received considerable attention owing to their numerous advantages such as high removal efficiency of suspended solids and lower footprints. Low-pressure membrane filtration has been widely used for the removal of pathogens, suspended particulate matters, and certain organic matters from surface water, wastewater, and micro-polluted surface waters [1–4]. However, membrane fouling represents a serious issue for membrane filtration processes since it reduces the permeate production while increasing the operational costs and potentially leading to membrane deterioration.

Coagulation is a simple, low-cost, and efficient approach that has been widely applied for membrane fouling mitigation [5,6].

* Corresponding author.

Furthermore, numerous approaches (e.g., coagulation aid [7], preoxidation [8], and particle-activated carbon [9], among others) have been developed with the aim to enhance the efficiency of the coagulation process. In the last decade, numerous studies have shown that zero valent iron (ZVI) is highly efficient in degrading aquatic contaminants, although studies describing combined ZVI–coagulation processes are scarce in the literature. ZVI typically removes organic and inorganic contaminants by three main mechanisms (i.e., direct reduction, micro-electrolysis, and adsorption and precipitation) [10]. Direct reduction applications [11,12] have primarily focused on the electron-donating properties of ZVI. Thus, some metal ions or compounds are completely reduced by receiving electrons from ZVI, while other strong oxidation ions are partially reduced to less toxic species. The micro-electrolysis [13,14] applications take advantage of the electrochemical properties of ZVI. Thus, [H] and $Fe^{2+}$ (i.e., electrode reaction products) can perform oxidation–reduction reactions with numerous components present in wastewater, thereby greatly reducing the content of contaminants. For example, ZVI can promote the decomposition of a macromolecular material into a micromolecular intermediate or the transformation of non-biodegradable chemicals into tractable materials. In the adsorption and precipitation [15] applications, the high coagulation/adsorption capacity of ZVI is beneficial in that it promotes flocculation and precipitation during the corrosion process, thereby removing part of the contaminants by absorption. Therefore, ZVI can theoretically enhance the coagulation process.

Protein organic matter is responsible for significant membrane permeability losses [16,17]. Feng et al. [18] found that the degradation of proteins increased by 21.9% upon addition of ZVI during an anaerobic digestion process. Thus, membrane fouling caused by protein organic matter can be significantly mitigated via the addition of ZVI.

Additionally, the coagulation performance may change upon addition of particles. First, the particulate matter content and the collision efficiency can be increased. Second, the structure of the flocs can be modified such that the particles are entrapped within the flocs, thereby making them less compressible and more resistant to shear stress [19,20]. Finally, particle addition alters the cake layer structure making it less resistant and compressible [21,22]. Thus, membrane fouling can be mitigated by using the above approaches, and a ZVI–coagulation combined process may be used as a promising approach for enhancing coagulation while mitigating membrane fouling.

In this study, the performance of a polyvinylidene difluoride (PVDF) hollow fiber membrane during the ZVI particle-enhanced coagulation treatment of surface water was examined. The objectives of this combined technology were (1) to investigate the feasibility of applying ZVI in enhanced coagulation processes; (2) to explore the enhanced coagulation effect; and (3) to analyze the membrane fouling mitigation mechanisms.

## 2. Materials and methods

### 2.1. Characteristics of raw water

Raw water was collected from a micro-polluted surface water in Tianjin, China. The characteristics of the raw water are summarized in Table 1.

### 2.2. Materials

ZVI ($Fe^0$; Kermel, Tianjin, China) particles of ca. 90 µm in size (Fig. 1) were used in this study. Ferric chloride (Kermel, Tianjin, China) was chosen as a coagulant owing to its common usage as well as its ability to remove suspended matters during micro-polluted water treatments.

A PVDF hollow fiber membrane module (MOTIMO Membrane Technology, Tianjin, China) was used for each experiment. The effective surface area and the average pore size of the PVDF hollow fiber membrane were 0.058 $m^2$ and 0.1 µm, respectively.

### 2.3. Analytical methods

Total organic carbon (TOC), turbidity, $UV_{254}$ absorbance, and pH measurements were performed on a combustion-type organic carbon analyzer (TOC-VCPH analyzer, Shimadzu, Kyoto, Japan), a turbidimeter (2100N, Hach, Colorado, USA), an ultraviolet spectrophotometer (T6, PERSEE, Beijing, China), and a pH meter (PHS-25, Leici, China), respectively. The fractal dimension that characterizes the flocs was measured according to the methods developed by Wang et al. [23]. The flux decline was recorded with an electronic scale (CN-SE, Sakura, China). The ZVI particle and the floc sizes were measured on a laser particle analyzer (Mastersizer 2000, Malvern, Worcestershire, UK). Scanning electron microscopy

Table 1
Characteristics of raw water

| Parameter | Value |
|---|---|
| pH | 8.4 ± 0.7 |
| $UV_{254}$ (abs), $cm^{-1}$ | 0.134 ± 0.016 |
| TOC, mg/L | 32.46 ± 1.75 |
| $COD_{Mn}$, mg/L | 32.6 ± 1.68 |
| Turbidity, NTU | 11.5 ± 1.37 |
| $NH_3$–H, mg/L | 2.58 ± 0.24 |
| Temperature, °C | 20 ± 1 |
| Electrical conductivity, µs/cm | (0.196 ± 0.003) × $10^4$ |
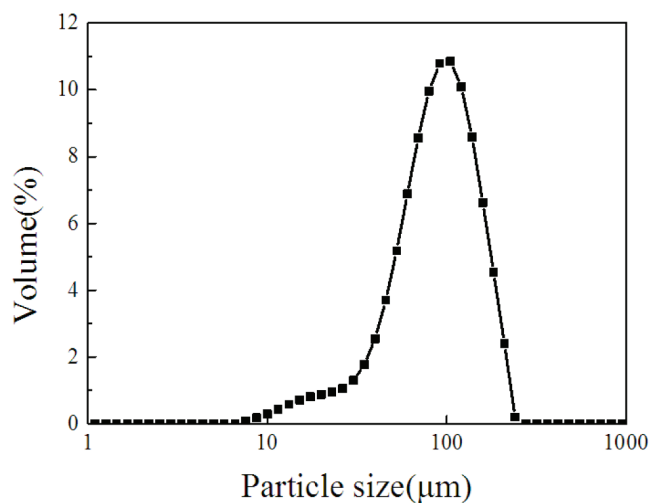


Fig. 1. Particle size distribution of zero valent iron ($Fe^0$, ZVI).

(SEM, XL30ESEM, Philips, Netherlands) was used to analyze the ZVI particles and the fouled membranes. Photographs of the flocs were taken by an industrial camera (MLM3XMP-CCD, China). The ferrous ion content was spectrophotometrically determined with 1,10-phenanthroline.

Fluorescence excitation–emission matrix (FEEM) measurements of the raw water and permeate samples were carried out on a fluorescence spectrophotometer (F-7000, Hitachi, Tokyo, Japan). The excitation and emission slits were set to a band-pass of 5 nm. The emission and excitation wavelengths were varied stepwise (5 nm intervals) from 250 to 500 nm and 200 to 400 nm, respectively. The characterization of the ZVI particles and the ZVI products was carried out by X-ray diffraction (XRD; Rigaku, D/MAX-2500, Japan).

### 2.4. Experimental operation

The bench-scale experimental setup used herein is shown in Fig. 2. The system consisted of coagulant solution, feeding, and permeate tanks as well as a membrane reactor.

The novel coagulant was prepared by mixing ZVI particles with a $FeCl_3$ coagulation solution in the coagulant solution tank. The concentrations of $FeCl_3$ and ZVI were 20 and 6 mg/L, respectively. The original membrane module was immersed in deionized water for 24 h before use. After each experimental cycle, the fouled membrane module was washed for 5 min (air–water backflushing; backwash pressure, 0.04 MPa; aeration intensity, 500 L/m²·min).

The permeate tank was used to collect the effluent from the membrane reactor. The tank was placed on an electronic counting scale to measure the mass of permeate, and the data were recorded on a computer.

For each experiment, a pristine membrane module was installed in the membrane reactor configured with an outside-in pressurization mode. First, the membrane module was pre-compacted by filtering deionized water for 1 h at constant pressure (0.02 MPa) and temperature (20 ± 1°C) until a constant permeate flux was achieved. After the pre-compaction step, the membrane filtration system was stopped and deionized water was removed from the membrane reactor. Subsequently, raw water mixed with the novel coagulant solution was continuously pumped into the membrane reactor. Once this process was finished, the membrane system was restarted and operated for a long time under the same operating conditions used during the pre-compaction run.

## 3. Results and discussion

### 3.1. Determination of the optimal dosage of ZVI

In a previous work, we aimed at determining the quality of water by using $FeCl_3$ as a coagulation agent at an optimal dosage of 20 mg/L. The determination of the optimum ZVI dosage was the main objective at this stage. The fractal dimension and the floc size were determined during the course of the experiment (Fig. 3(a)). These parameters are
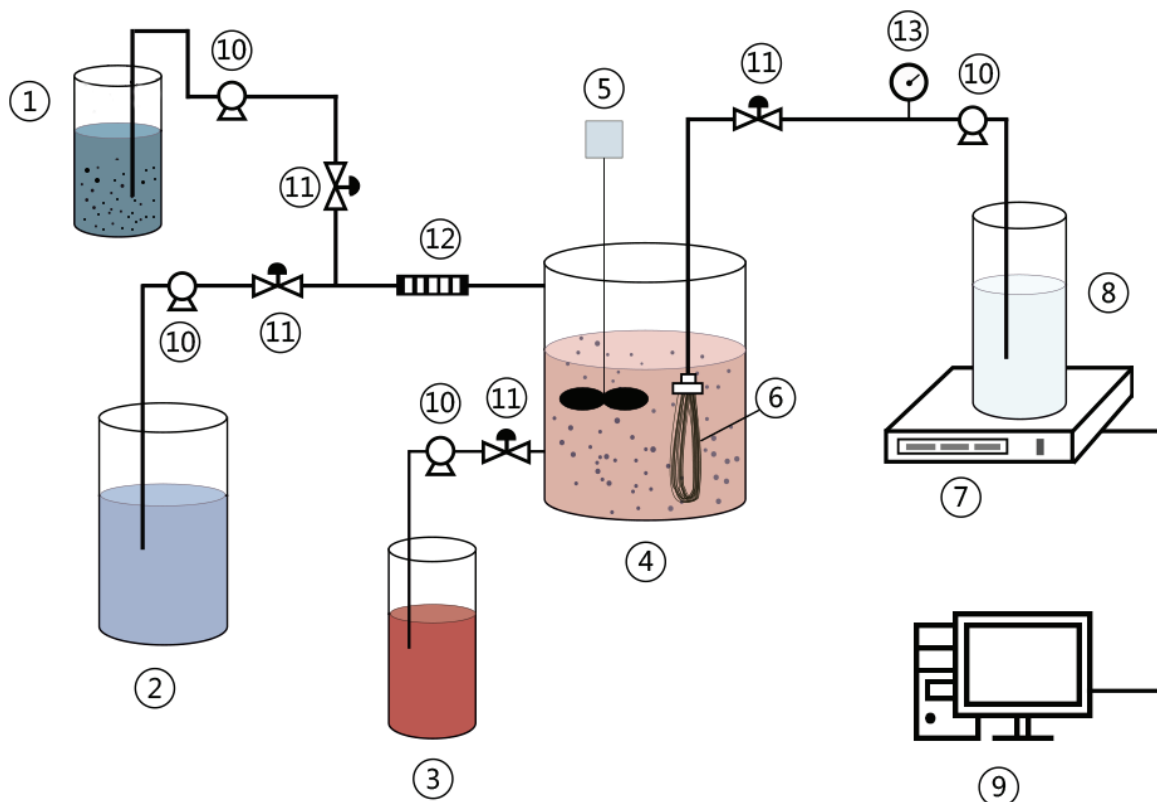


Fig. 2. Schematic diagram of experimental set up. (1) Coagulant solution tank; (2) feed tank; (3) concentrate collector; (4) membrane reactor; (5) blender; (6) membrane; (7) electronic balance; (8) permeate tank; (9) computer; (10) pump; (11) valve; (12) mixer unit; (13) vacuum meter.

important in that they can influence the subsequent membrane fouling process. Thus, larger fractal dimensions (i.e., flocs with irregular shape) and floc sizes are beneficial for membrane fouling mitigation [24,25]. Additionally, we monitored various effluent parameters such as TOC, chemical oxygen demand (COD), ammonia nitrogen concentration, and $UV_{254}$ (Fig. 3(b)) to ensure effluent quality.

As shown in Fig. 3(a), the fractal dimension remained stable for ZVI dosages of 6–9 mg/L and decreased thereafter (ZVI dosages higher than 9 mg/L). The floc size achieved larger and relatively stable values at ZVI dosages of 6–9 mg/L. As shown in Fig. 3(b), ZVI dosages of 6–9 mg/L allowed effluents with excellent quality in terms of TOC, COD, ammonia nitrogen concentration, and $UV_{254}$. Considering the efficiency and economic cost of the treatment, a ZVI dosage of 6 mg/L was used for subsequent studies. Additionally, in virtue of the stable effluent quality obtained, we can conclude that neither ZVI nor the formed flocs damaged the surface of the membrane.

### 3.2. Membrane fouling and effluent quality

The TOC, $COD_{Mn}$, and $UV_{254}$ removal efficiencies of different combined membrane technologies are represented in Fig. 4. The results indicated that the addition of ZVI at 6 mg/L increased the TOC, $COD_{Mn}$, and $UV_{254}$ removal efficiencies by 5.4%, 13.7%, and 23.1%, respectively. The observed removal

of organic compounds can be explained by (1) coagulation of tiny suspended particles and colloids to form larger flocs then are subsequently settled; (2) membrane interception resulted in rejection of particles and impurities (even with sizes lower than the membrane pore size); and (3) addition of ZVI, the dominant factor in this study. The large specific surface area and high surface activity of ZVI allow this compound to adsorb a fraction of the organic matters. Moreover, the reductive characteristics of ZVI are beneficial in that organic matters can be more efficiently removed via oxidation–reduction reactions.

Constant-pressure flux decline tests were performed to investigate the membrane fouling process. The evolution of the normalized flux ($J/J_0$) during filtration is shown in Fig. 5. The addition of ZVI resulted in lower flux decays after three operation cycles. Thus, the ZVI–coagulation combined and the conventional coagulation membrane processes showed final $J/J_0$ values of 0.38 and 0.24, respectively. After the first
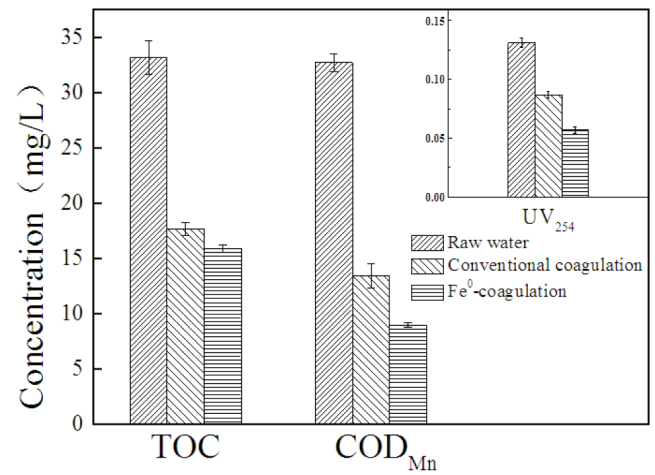


Fig. 4. Removal efficiencies of TOC, $COD_{Mn}$, and $UV_{254}$ in the process of conventional coagulation membrane filtration and ZVI–coagulation membrane filtration.



Fig. 3. The determination of optimal dosage.
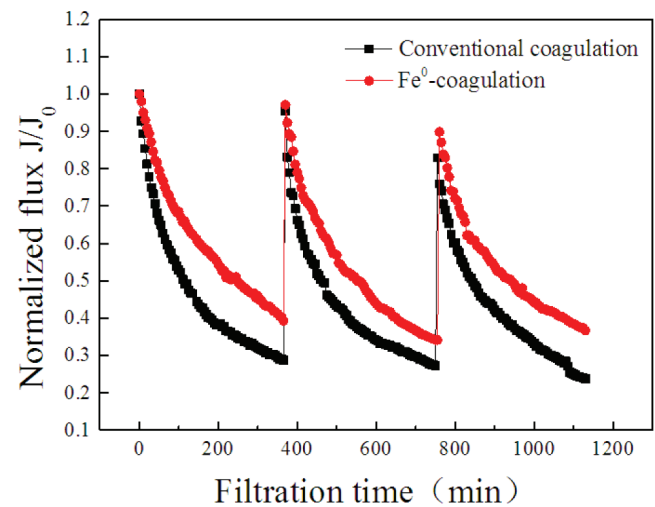


Fig. 5. Normalized flux variations of conventional coagulation membrane filtration and ZVI–coagulation membrane filtration process.

physical cleaning, the initial $J/J_0$ for both processes differed by 0.04 units (ZVI–coagulation membrane: 0.97; conventional coagulation membrane: 0.93). However, after the second physical cleaning, the combined process showed a restored initial $J/J_0$ value of 0.91 (vs. 0.83 for the conventional membrane process). Thus, higher flux recovery values were obtained for the combined process after the second cycle. The results can be explained in terms of ZVI addition enhancing the efficiency of coagulation. Second, the larger floc sizes obtained during the coagulation process upon ZVI addition effectively resulted in a looser cake layers and lower membrane filtration resistances [26]. Furthermore, the content of particles and the probability of collision increased upon addition of ZVI, thereby favoring the formation of loose flocs with higher movement abilities and the building of a highly porous cake layer. This porous cake layer can intercept colloidal particles, thereby preventing them from depositing on the surface and into the pores of the membrane.

### 3.3. Characterization of ZVI and the ZVI–coagulation products

Different surface textures of ZVI were revealed by the SEM images (Fig. 6). The rough and uneven surface of ZVI was indicative of a large specific surface area material allowing more efficient oxidation–reduction reactions. After the oxidation–reduction reaction, the surface of ZVI was roughish and relatively dense as a result of corrosion products covering the surface and filling the surface ravines. As revealed by X-ray diffraction (XRD; Fig. 7), ZVI was still present after the reaction, although the diffraction peaks corresponding to ZVI were less intense and new peaks ascribed to magnetite/maghemite (M; $Fe_3O_4/\gamma$-$Fe_2O_3$) and lepidocrocite (L; $\gamma$-FeOOH) phases were observed.

As shown in Fig. 7(a), three major peaks ascribed to ZVI were observed at 45°, 65°, and 85° in agreement with previously reported nano- and micro-sized ZVI particles [27,28]. According to the X-ray diffractograms, the ZVI corrosion products were composed of a mixture of amorphous iron(III) oxide/hydroxide, magnetite ($Fe_3O_4$) and/or maghemite ($\gamma$-$Fe_2O_3$), and lepidocrocite ($\gamma$-FeOOH) [29,30]. Thus, ZVI underwent a clear structural transformation as a result of the coagulation treatment. The presence of Fe(II)/(III) and Fe(III) corrosion products revealed that Fe(II) was an intermediate species in the ZVI corrosion process [28].

ZVI reacts with $H_2O$ or $O_2$ to release $Fe^{2+}$ and $OH^-$ [31]. $Fe^{2+}$ further precipitates in the form of $Fe(OH)_2$ upon reaction with $H_2O$, $O_2$, or $OH^-$ [28]. These processes are described in the following equations:

$$Fe^0 + 2H_2O \rightarrow 2Fe^{2+} + H_2 + 2OH^- \tag{1}$$

$$Fe^0 + O_2 + 2H_2O \rightarrow 2Fe^{2+} + 4OH^- \tag{2}$$

$$6Fe^{2+} + O_2 + 6H_2O \rightarrow 2Fe_3O_4(s) + 12H^+ \tag{3}$$

$$Fe^{2+} + 2OH^- \rightarrow Fe(OH)_2(s) \tag{4}$$
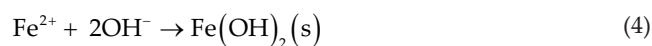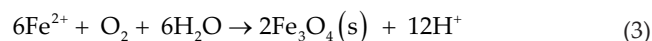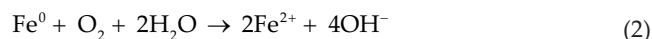
Through this process, the ZVI system can take advantage of both reductive and oxidative reactions, thereby increasing the versatility of this technology. Reductive and oxidative reactions may lead to the removal of pollutants responsible for membrane fouling, and this would explain the lower flux decline and the membrane fouling mitigation characteristics of the combined process.

In order to verify the evolution of the ZVI particles, the release of $Fe^{2+}$ species in this process was investigated
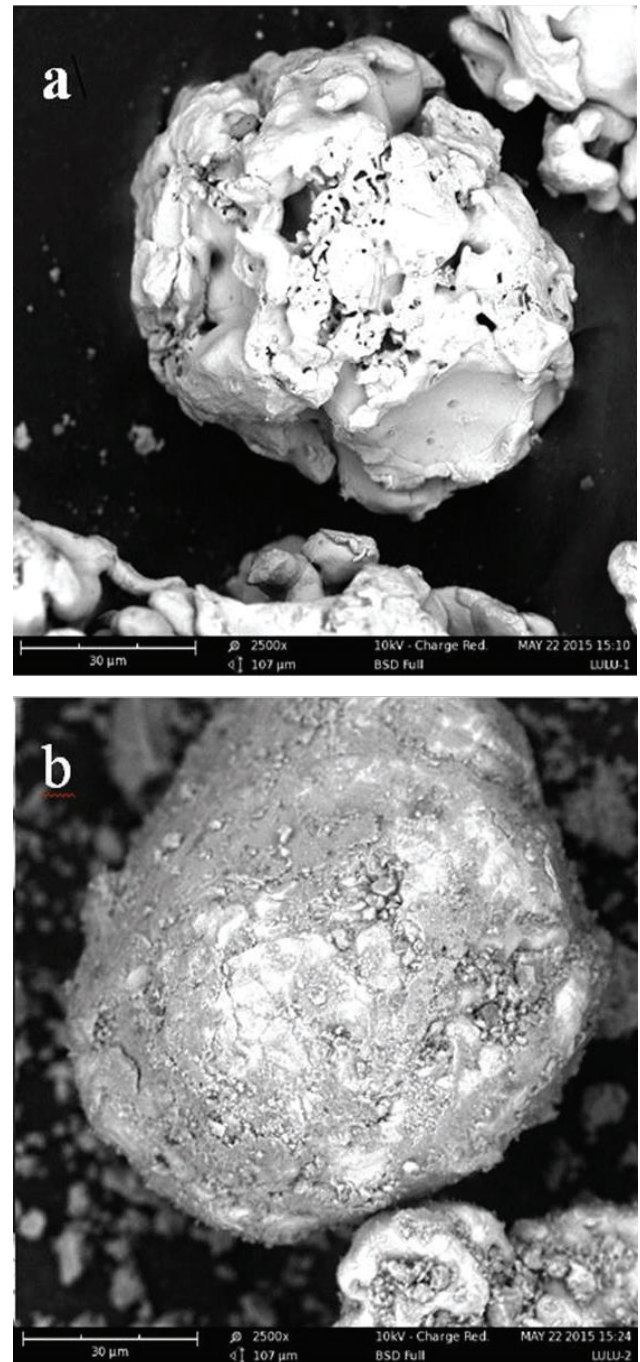


Fig. 6. SEM image of ZVI: (a) original ZVI particle and (b) ZVI particle in ZVI–coagulation membrane filtration process. $FeCl_3$ dosage in each process was 20 mg/L.

(Fig. 8). In the presence of ZVI particles, the concentration of $Fe^{2+}$ was noticeably higher, although a lag period was observed in the process. This initial lag period was generally believed to be associated with (1) the formation of secondary reductants before the contaminants are reduced and (2) the removal of the iron oxide layer [32–34]. Ferrous iron is an unstable and reactive ion that intensifies the effect of the oxidation–reduction processes.

### 3.4. Three-dimensional fluorescence

FEEM spectroscopy has been widely used to characterize dissolved organic matter (DOM) in water and soil since it allows to distinguish different DOM species with diverse origins [35]. Organic matter (e.g., humic acid [HA], fulvic acid [FA], or protein) can be categorized by analyzing the shapes and peaks of the FEEM contour map. Excitation and emission boundaries are typically defined as follows. Regions I and II belonged to simple aromatic proteins such as tyrosine, region III corresponded to FA-like substances, region IV corresponded to soluble microbial by-product-like (SMP-like)

substances, and region V was indicative of HA-like compounds [35,36]. The FEEM spectrum (Fig. 9(a)) qualitatively indicated the DOM composition of the raw water sample. The peaks or shoulders in regions I, II, III, IV, and V (four peaks:
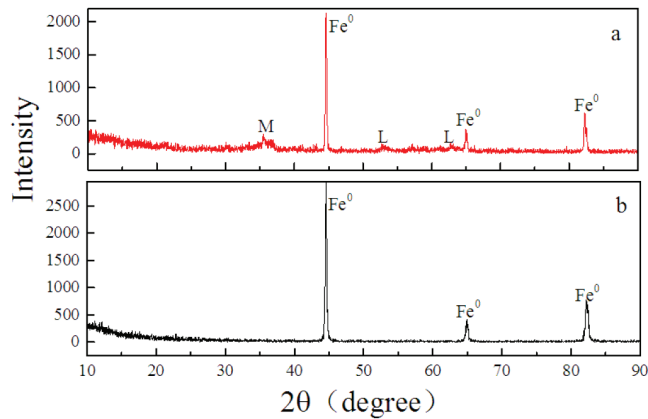


Fig. 7. X-ray diffraction analysis of ZVI: (a) ZVI particle in ZVI–coagulation membrane filtration process and (b) ZVI particle. Peaks are referred to magnetite/maghemite (M; $Fe_3O_4/\gamma$-$Fe_2O_3$), lepidocrocite (L; $\gamma$-FeOOH) and ZVI, respectively.
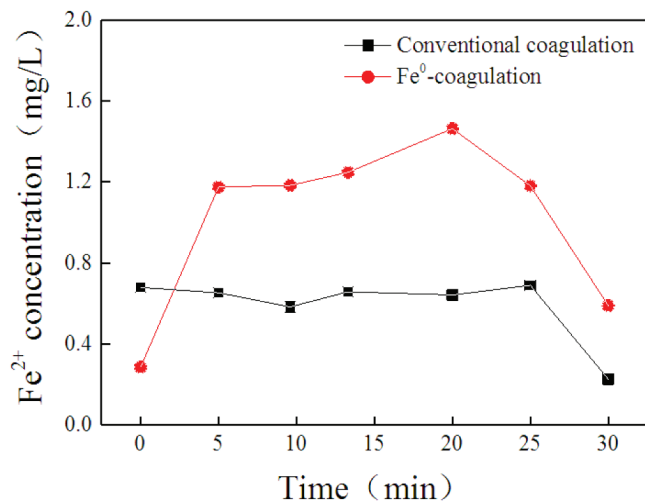


Fig. 8. The variation of $Fe^{2+}$ concentration in the process.
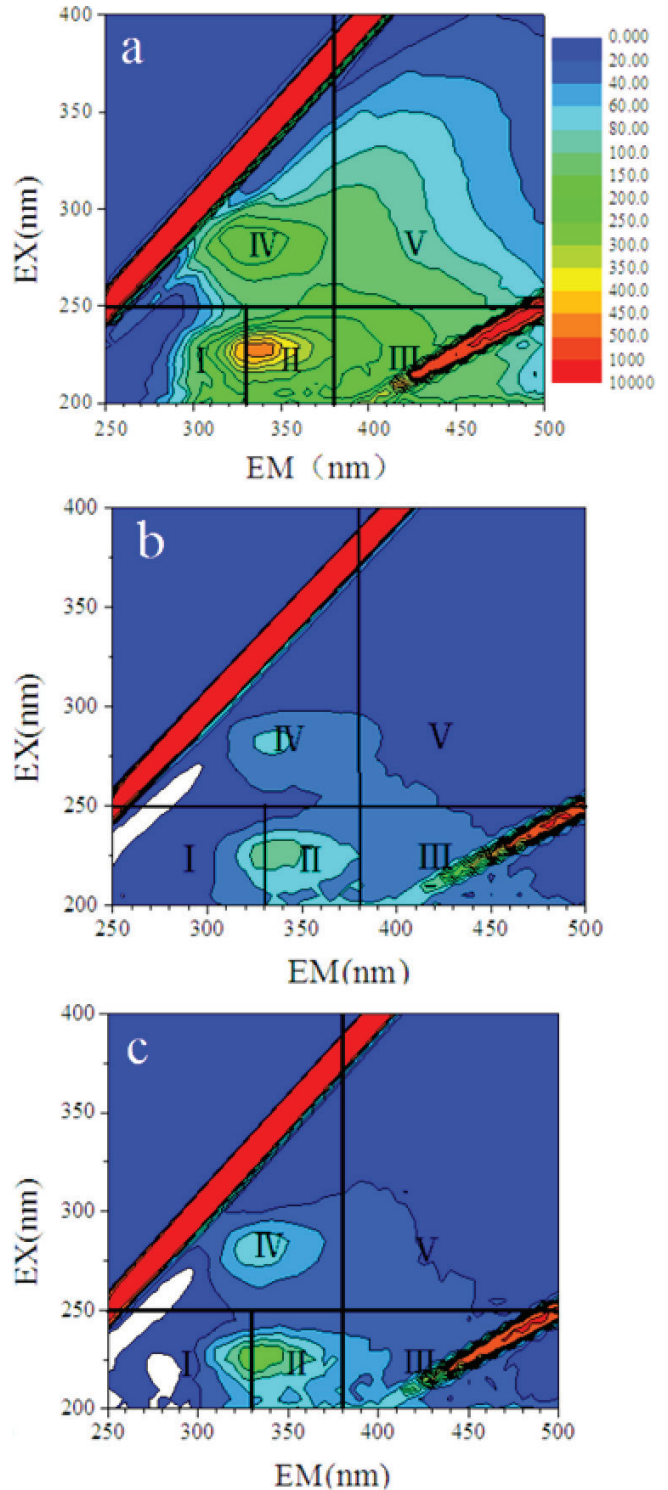


Fig. 9. FEEM of (a) the raw water, (b) subtraction spectrum after conventional coagulation membrane filtration process, and (c) subtraction spectrum after ZVI–coagulation membrane filtration process.

Ex = 220–240, Em = 330–350; Ex = 210–220, Em = 410–430; Ex = 260–280, Em = 320–350; and Ex = 300–320, Em = 390–410) were indicative of the presence of protein, FA-like, SMP-like, and HA-like substances.

The subtraction spectra of the ZVI–coagulation and conventional coagulation processes are shown in Figs. 9(b) and (c), respectively. By comparing both spectra, it is clear that protein and SMP-like substances were mostly removed after the ZVI–coagulation process, while the conventional coagulation process only removed a fraction of these compounds. Protein organic matter is one of the compounds producing rapid flux decline during membrane filtration processes [37]. Since the addition of ZVI particles achieved more efficient removal of protein substances, this process was effective in mitigating membrane fouling caused by protein substances.

### 3.5. Floc characterization

Fig. 10 shows some images of the flocs formed during the conventional- and ZVI–coagulation processes. The ZVI–coagulation process generated larger and looser flocs as compared with the conventional coagulation technology.
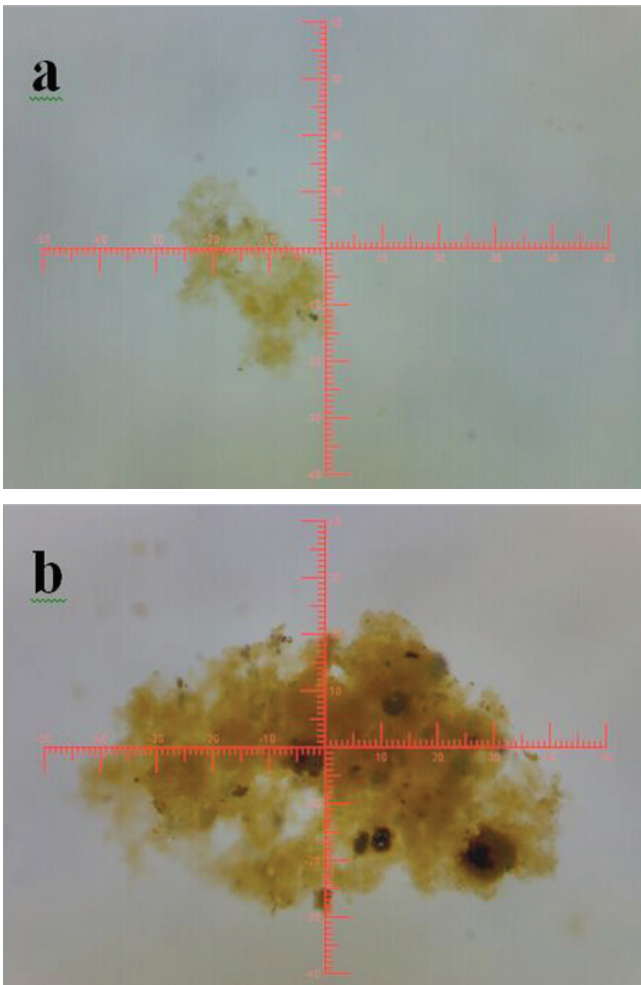
Fig. 10. Images of flocs in different process: (a) conventional coagulation and (b) ZVI–coagulation. FeCl$_3$ dosage in each process was 20 mg/L.

As shown in Fig. 10(b), the ZVI particles were unevenly distributed in the flocs.

Fig. 11 shows that the floc size distributions for both conventional coagulation and ZVI–coagulation membrane filtration processes. The ZVI–coagulation process showed larger floc particle sizes as compared with the conventional coagulation technology (average particle size: 523.215 vs. 264.482 mm).

According to the Kozeny–Carman theory [38], the specific resistance of a cake layer could be expressed as follows:

$$r_c = 180 \frac{(1-\varepsilon)^3}{[(d_s)^2 \varepsilon^3]} \tag{5}$$

where $\gamma_c$ is the resistance of the cake layer, $d_s$ is the diameter of the particle (m), and $\varepsilon$ is the porosity of the cake layer (%). The specific resistance of a cake layer decreases with the floc particle size.

Huang et al., Wang et al., and Howe et al. [39–41] investigated the relationship between the floc particle size and the membrane fouling phenomenon. These authors demonstrated that membrane fouling can be mitigated by increasing the floc particle size to a certain extent. Herein, the addition of ZVI particles dramatically increased the floc size, thereby mitigating membrane fouling to a certain extent.

Furthermore, as pointed out by recent studies, the total filtration resistance of a foulant layer involves hydraulic (described by the Kozeny–Carman theory) and osmotic pressure-induced resistance terms [42–44]. The osmotic pressure-induced resistance is mainly caused by extracellular polymeric substances, SMPs, and biopolymer clusters. As described in sections 3.2 and 3.4, protein and SMP-like substances (similar to SMPs) were mostly and partly removed by the ZVI–coagulation and conventional coagulation processes, respectively. Thus, the osmotic pressure-induced resistance can be reduced via the ZVI–coagulation process.

Thereafter, the total filtration resistance of a foulant layer can be effectively mitigated during the ZVI–coagulation membrane process.
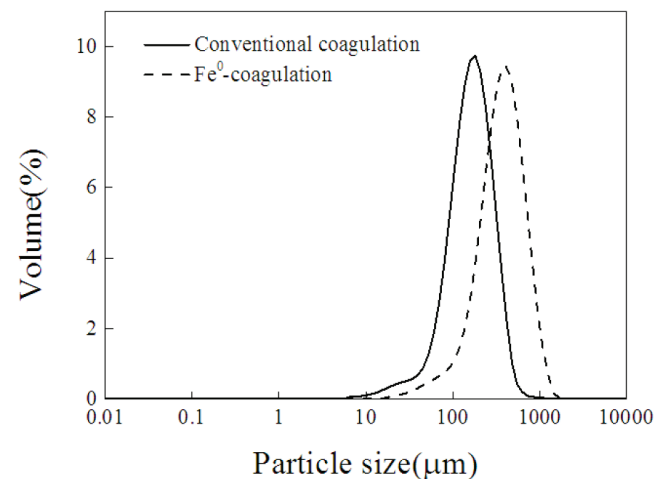
Fig. 11. Particle size distribution in different processes.

### 3.6. SEM observations of the cake layer

SEM images of some PVDF hollow fiber membrane samples after filtration are shown in Fig. 12. The properties of the flocs determined the morphology of the cake layer. The cake layers generated after conventional coagulation and ZVI–coagulation membrane processes were compared. Thus, the conventional coagulation membrane filtration process generated a relatively smooth cake layer with a dense structure and low porosity. In contrast, the ZVI–coagulation membrane filtration process resulted in a rough, permeable, and porous cake layer. Additionally, the ZVI particles
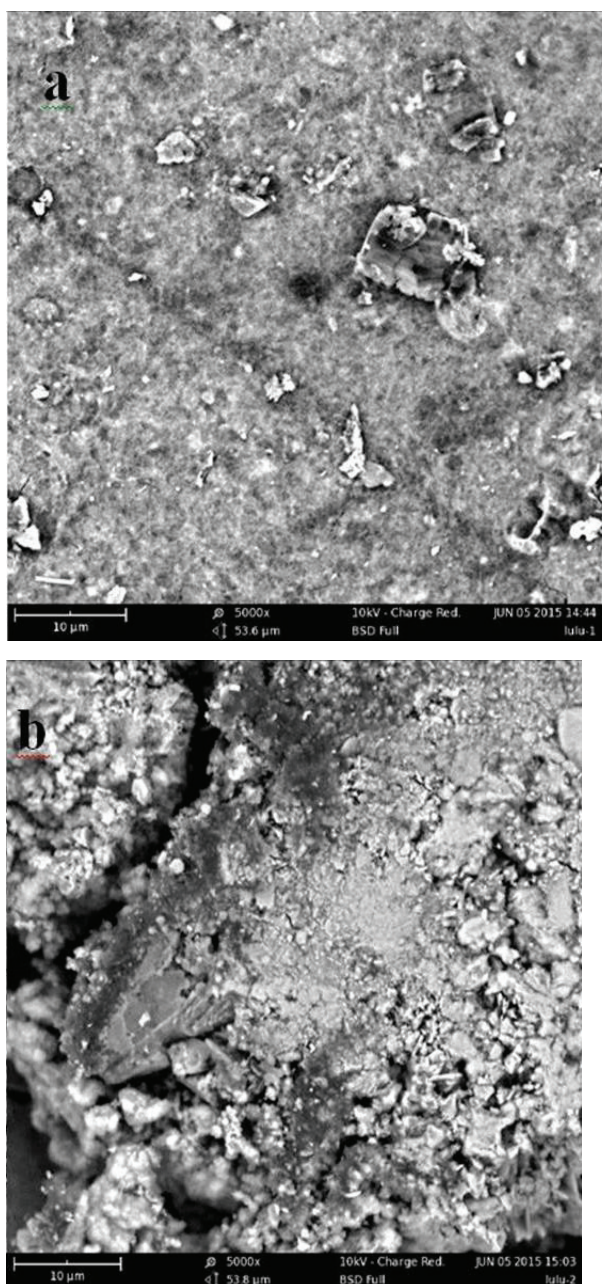


Fig. 12. SEM images of cake layer: (a) conventional coagulation membrane filtration process and (b) ZVI–coagulation membrane filtration process. FeCl$_3$ dosage in each process was 20 mg/L.

were randomly distributed on the surface of the cake layer serving as a support. Thus, the ZVI particles can make the cake layer to be relatively loose, increasing its porosity and water transmittance characteristics, and mitigating membrane fouling as a result.

By combining floc size and SEM analyses, denser and smaller flocs were found to easily block the membrane pores, leading to unsupported cake layers with a relatively compact structure. Densification of the cake layer resulted in lower porosity and rapid flux drops. The presence of large size flocs can reduce the likelihood of small particles blocking the membrane pores during the initial stages of ZVI–coagulation membrane filtration. Furthermore, the support of the ZVI particles and the interaction between the ZVI-flocs and the membrane surface resulted in cake layers with enhanced porosity and water permeability characteristics, thereby mitigating membrane fouling.

### 4. Conclusions

A ZVI coagulation membrane filtration process was developed herein. The ZVI–coagulation membrane filtration process allowed to significantly reduce the TOC, COD$_{Mn}$, and UV$_{254}$ parameters as compared with conventional coagulation membrane filtration. Additionally, the ZVI–coagulation membrane filtration technology significantly mitigated membrane fouling as compared with conventional coagulation membrane filtration. As revealed by FEEM, XRD, and SEM, ZVI reacted and possibly remove or absorb a fraction of the contaminants. During the membrane filtration process, the ZVI technology resulted in larger and looser flocs leading to the deposition of looser and more permeable cake layers on the membrane surface. Thus, the performance of the coagulation process was enhanced and the membrane fouling phenomena were mitigated. We believe that the ZVI–coagulation membrane technology developed herein will provide a new alternative to scientists working in the field of micro-polluted surface water treatment.

### Acknowledgments

### References

[1] H. Guo, Y. Wyart, J. Perot, F. Nauleau, P. Moulin, Low-pressure membrane integrity tests for drinking water treatment: a review, Water Res., 44 (2010) 41–57.

[2] C. Ma, S. Yu, W. Shi, W. Tian, S.G.J. Heijman, L.C. Rietveld, High concentration powdered activated carbon-membrane bioreactor (PAC-MBR) for slightly polluted surface water treatment at low temperature, Bioresour. Technol., 113 (2012) 136–142.

[3] C. Ma, S. Yu, W. Shi, S.G.J. Heijman, L.C. Rietveld, Effect of different temperatures on performance and membrane fouling in high concentration PAC-MBR system treating micro-polluted surface water, Bioresour. Technol., 141 (2013) 19–24.

[4] Q. Li, Z.Q. Yan, X.L. Wang, A poly(sulfobetaine) hollow fiber ultrafiltration membrane for the treatment of oily wastewater, Desal. Wat. Treat., 57 (2016) 11048–11065.

[5] M. Yao, J. Nan, Q. Li, D. Zhan, T. Chen, Z. Wang, H. Li, Effect of under-dosing coagulant on coagulation-ultrafiltration process for treatment of humic-rich water with divalent calcium ion, J. Membr. Sci., 495 (2015) 37–47.

[6] G. Masmoudi, E. Ellouze, R. Ben Amar, Hybrid coagulation/membrane process treatment applied to the treatment of industrial dyeing effluent, Desal. Wat. Treat., 57 (2016) 6781–6791.

[7] Y. Wang, N. Xue, Y. Chu, Y. Sun, H. Yan, Q. Han, CuO nanoparticle-humic acid (CuONP-HA) composite contaminant removal by coagulation/ultrafiltration process: the application of sodium alginate as coagulant aid, Desalination, 367 (2015) 265–271.

[8] P. Xie, Y. Chen, J. Ma, X. Zhang, J. Zou, Z. Wang, A mini review of preoxidation to improve coagulation, Chemosphere, 155 (2016) 550–563.

[9] Y. Bao, J. Niu, Z. Xu, D. Gao, J. Shi, X. Sun, Q. Huang, Removal of perfluorooctane sulfonate (PFOS) and perfluorooctanoate (PFOA) from water by coagulation: mechanisms and influencing factors, J. Colloid Interface Sci., 434 (2014) 59–64.

[10] X. Guan, Y. Sun, H. Qin, J. Li, I.M.C. Lo, D. He, H. Dong, The limitations of applying zero-valent iron technology in contaminants sequestration and the corresponding countermeasures: the development in zero-valent iron technology in the last two decades (1994–2014), Water Res., 75 (2015) 224–248.

[11] B. Calderon, A. Fullana, Heavy metal release due to aging effect during zero valent iron nanoparticles remediation, Water Res., 83 (2015) 1–9.

[12] F. Fu, D.D. Dionysiou, H. Liu, The use of zero-valent iron for groundwater remediation and wastewater treatment: a review, J. Hazard. Mater., 267 (2014) 194–205.

[13] L. Zhang, L. Zhang, D. Li, Enhanced dark fermentative hydrogen production by zero-valent iron activated carbon micro-electrolysis, Int. J. Hydrogen Energy, 40 (2015) 12201–12208.

[14] J. Luo, G. Song, J. Liu, G. Qian, Z.P. Xu, Mechanism of enhanced nitrate reduction via micro-electrolysis at the powdered zero-valent iron/activated carbon interface, J. Colloid Interface Sci., 435 (2014) 21–25.

[15] Z.J. Li, L. Wang, L.Y. Yuan, C.L. Xiao, L. Mei, L.R. Zheng, J. Zhang, J.H. Yang, Y.L. Zhao, Z.T. Zhu, Z.F. Chai, W.Q. Shi, Efficient removal of uranium from aqueous solution by zero-valent iron nanoparticle and its graphene composite, J. Hazard. Mater., 290 (2015) 26–33.

[16] W. Yu, N. Graham, Y. Yang, Z. Zhou, L.C. Campos, Effect of sludge retention on UF membrane fouling: the significance of sludge crystallization and EPS increase, Water Res., 83 (2015) 319–328.

[17] L.Y. Wong, C.A. Ng, M.J.K. Bashir, C.K. Cheah, K.L. Khoo, Y.C. Ching, Membrane bioreactor performance improvement by adding adsorbent and coagulant: a comparative study, Desal. Wat. Treat., 57 (2016) 13433–13439.

[18] Y. Feng, Y. Zhang, X. Quan, S. Chen, Enhanced anaerobic digestion of waste activated sludge digestion by the addition of zero valent iron, Water Res., 52 (2014) 242–250.

[19] J.C. Lee, J.S. Kim, I.J. Kang, M.H. Cho, P.K. Park, C.H. Lee, Potential and limitations of alum or zeolite addition to improve the performance of a submerged membrane bioreactor, Water Sci. Technol., 43 (2001) 59–66.

[20] P. Loulergue, M. Weckert, B. Reboul, C. Cabassud, W. Uhl, C. Guigui, Mechanisms of action of particles used for fouling mitigation in membrane bioreactors, Water Res., 66 (2014) 40–52.

[21] B. Teychene, C. Guigui, C. Cabassud, Engineering of an MBR supernatant fouling layer by fine particles addition: a possible way to control cake compressibility, Water Res., 45 (2011) 2060–2072.

[22] S. Jamal Khan, C. Visvanathan, V. Jegatheesan, Effect of powdered activated carbon (PAC) and cationic polymer on biofouling mitigation in hybrid MBRs, Bioresour. Technol., 113 (2012) 165–168.

[23] J. Wang, J. Yang, H. Zhang, W. Guo, H.H. Ngo, Feasibility study on magnetic enhanced flocculation for mitigating membrane fouling, J. Ind. Eng. Chem., 26 (2015) 37–45.

[24] P.K. Park, C.H. Lee, S. Lee, Determination of cake porosity using image analysis in a coagulation-microfiltration system, J. Membr. Sci., 293 (2007) 66–72.

[25] L. Ehrl, M. Soos, M. Morbidelli, Dependence of aggregate strength, structure, and light scattering properties on primary particle size under turbulent conditions in stirred tank, Langmuir, 24 (2008) 3070–3081.

[26] S. Kim, H. Park, Effective diameter for shear-induced diffusion for characterizing cake formation in crossflow microfiltration at polydisperse conditions, J. Environ. Eng., 131 (2005) 865–873.

[27] J.T. Nurmi, P.G. Tratnyek, V. Sarathy, D.R. Baer, J.E. Amonette, K. Pecher, C. Wang, J.C. Linehan, D.W. Matson, R.L. Penn, M.D. Driessen, Characterization and properties of metallic iron nanoparticles: spectroscopy, electrochemistry, and kinetics, Environ. Sci. Technol., 39 (2005) 1221–1230.

[28] S.R. Kanel, B. Manning, L. Charlet, H. Choi, Removal of arsenic(III) from groundwater by nanoscale zero-valent iron, Environ. Sci. Technol., 39 (2005) 1291–1298.

[29] A. Khan, S.M. Prabhu, J. Park, W. Lee, C.M. Chon, J.S. Ahn, G. Lee, Azo dye decolorization by ZVI under circum-neutral pH conditions and the characterization of ZVI corrosion products, J. Ind. Eng. Chem., 47 (2017) 86–93.

[30] Z. Yang, C. Shan, W. Zhang, Z. Jiang, X. Guan, B. Pan, Temporospatial evolution and removal mechanisms of As(V) and Se(VI) in ZVI column with $H_2O_2$ as corrosion accelerator, Water Res., 106 (2016) 461–469.

[31] S.M. Ponder, J.G. Darab, T.E. Mallouk, Remediation of Cr(VI) and Pb(II) aqueous solutions using supported, nanoscale zero-valent iron, Environ. Sci. Technol., 34 (2000) 2564–2569.

[32] M.J. Alowitz, M.M. Scherer, Kinetics of nitrate, nitrite, and Cr(VI) reduction by iron metal, Environ. Sci. Technol., 36 (2002) 299–306.

[33] A.D. Bokare, W. Choi, Zero-valent aluminum for oxidative degradation of aqueous organic pollutants, Environ. Sci. Technol., 43 (2009) 7130–7135.

[34] L. Liang, W. Sun, X. Guan, Y. Huang, W. Choi, H. Bao, L. Li, Z. Jiang, Weak magnetic field significantly enhances selenite removal kinetics by zero valent iron, Water Res., 49 (2014) 371–380.

[35] W. Chen, P. Westerhoff, J.A. Leenheer, K. Booksh, Fluorescence excitation-emission matrix regional integration to quantify spectra for dissolved organic matter, Environ. Sci. Technol., 37 (2003) 5701–5710.

[36] H. Yamamura, K. Okimoto, K. Kimura, Y. Watanabe, Hydrophilic fraction of natural organic matter causing irreversible fouling of microfiltration and ultrafiltration membranes, Water Res., 54 (2014) 123–136.

[37] Z. Liu, B.Z. Dong, Y. Chen, H. Liu, Characterization of membrane fouling by three-dimension fluorescence excitation, Environ. Chem., 29 (2010) 496–501.

[38] M. Mulder, Basic Principles of Membrane Technology, Kluwer Academic Publishers, London, UK, 1991.

[39] K.J. Howe, A. Marwah, K.P. Chiu, S.S. Adham, Effect of coagulation on the size of MF and UF membrane foulants, Environ. Sci. Technol., 40 (2006) 7908–7913.

[40] X. Wang, L. Wang, Y. Liu, W. Duan, Ozonation pretreatment for ultrafiltration of the secondary effluent, J. Membr. Sci., 287 (2007) 187–191.

[41] H. Huang, R. Spinette, C.R. O'Melia, Direct-flow microfiltration of aquasols. I. Impacts of particle stabilities and size, J. Membr. Sci., 314 (2008) 90–100.

[42] H. Hong, M. Zhang, Y. He, J. Chen, H. Lin, Fouling mechanisms of gel layer in a submerged membrane bioreactor, Bioresour. Technol., 166 (2014) 295–302.

[43] J. Chen, M. Zhang, F. Li, L. Qian, H. Lin, L. Yang, X. Wu, X. Zhou, Y. He, B.Q. Liao, Membrane fouling in a membrane bioreactor: high filtration resistance of gel layer and its underlying mechanism, Water Res., 102 (2016) 82–89.

[44] L. Zhao, F. Wang, X. Weng, R. Li, X. Zhou, H. Lin, H. Yu, B.Q. Liao, Novel indicators for thermodynamic prediction of interfacial interactions related with adhesive fouling in a membrane bioreactor, J. Colloid Interface Sci., 487 (2017) 320–329.